

## Cross sections for excitation of atomic hydrogen to the $n = 2, 3,$ and $4$ states by 15–200-keV protons\*

J. T. Park, J. E. Aldag, J. M. George, and J. L. Peacher

*Department of Physics, University of Missouri-Rolla, Rolla, Missouri 65401*

(Received 22 March 1976)

Cross sections for the processes  $H^+ + H(1s) \rightarrow H^+ + H^*(n = 2, 3, 4)$  have been extracted from the energy-loss spectra of 15- to 200-keV protons by using a spectrum-fitting technique. Absolute cross sections have been obtained by normalization of the spectra to the theoretical cross section through the use of the Born approximation at 200 keV. The cross-section curves are very similar in shape with maxima at 60 keV. The results have been compared with available theoretical calculations. The  $n = 2$  and  $n = 3$  cross-section measurements are in very good agreement in curve shape with Glauber-approximation calculations.

### I. INTRODUCTION

The scattering of a proton by a hydrogen atom is one of the most fundamental reactions in atomic physics. This system is used to compare various scattering approximations, because both the internal structure of hydrogen and the interaction of the hydrogen atom with the incident proton are known. However, it has not been possible to choose among the various theoretical approaches in the intermediate- to high-impact-energy range, because the number of experimental measurements of cross sections is very sparse. The measurements reported here for excitation by proton impact of atomic hydrogen from the ground state to the  $n = 2, 3,$  and  $4$  states will make it possible to compare theoretical scattering approximations with experiments in the intermediate- to high-energy range. They will make it possible to ascertain the usefulness of a particular theoretical scattering approximation.

Until recently, the low-energy measurements of excitation of the  $n = 2$  levels<sup>1-4</sup> obtained using crossed-beam techniques were the only ones available for excitation of atomic hydrogen. Measurements of the excitation to the  $n = 2$  state using the energy-loss technique at a wide range of impact energies were published in 1975 by Park *et al.*<sup>5</sup> The present effort extends the measurements to the  $n = 3$  and  $n = 4$  states, and additional data are presented for the  $n = 2$  excitation.

The investigation is based on an energy-loss spectrometry method.<sup>5-9</sup> The cross sections were obtained from analysis of the energy-loss spectra of scattered protons which had traversed a target furnace containing atomic hydrogen. This energy-loss technique avoids problems in the crossed-beam technique which make it difficult to extend crossed-beam measurements into the intermediate-energy range.

### II. EXPERIMENTAL METHOD

The energy-loss spectrometer at the University of Missouri-Rolla, and the general method employed in ion energy-loss spectrometry have been discussed in detail elsewhere.<sup>5-9</sup> In the current experiment, protons produced in a low-voltage discharge source are focused and mass analyzed by a Wien filter. The mass-selected protons are accelerated and steered through a target furnace chamber constructed of tungsten tubes. After traversing the scattering chamber, the protons pass through an exit collimator, and the transmitted beam is magnetically analyzed to remove any products of charge exchange. Beyond the magnet, the protons are decelerated by a well-defined potential and analyzed by a  $127^\circ$  electrostatic energy analyzer.

Spectra differential in energy loss are obtained by increasing  $\Delta V$ , the potential between the accelerator and decelerator terminals. Whenever the increased potential energy compensates for a discrete energy loss of the proton-atomic-hydrogen collision system, a peak is detected in the spectrum. The energy-loss scale can be determined to an accuracy of  $\pm 0.03$  eV.<sup>8</sup>

To obtain atomic hydrogen, a high-temperature furnace is required. The target furnace is constructed of coaxial tungsten tubes. Current flows radially into one end of the furnace, flows coaxially through the wall of the furnace, returns through an adjacent coaxial shield, and finally flows radially outward. The copper plates carrying the current radially to and from the furnace are only 0.25 cm apart. The proton beam is directed coaxially through the center of the furnace. The calculated magnetic field along the furnace axis is zero. We have not been able to detect any effect from magnetic fields produced by currents in the furnace.

The proton beam enters and leaves the furnace through holes in the ends of thin-walled tungsten cones. These cones are attached to the copper blocks holding the furnace. This arrangement is very rigid and has a low heat conductivity. It does not move as the furnace is heated even if some sagging occurs in the furnace itself.

Gas entering the target furnace is introduced between the furnace wall and the heated coaxial shield. Because both the furnace and the shield are heated, the gas is partially dissociated before it enters the furnace. The furnace is connected to a tube leading to a MKS Baratron pressure meter. The output of the pressure meter is fed to a pressure regulator, which serves to maintain a constant pressure in the chamber.

The atomic-hydrogen pressure in the furnace cannot be accurately determined from the molecular-hydrogen pressure at the pressure meter, because the information on the temperature at various points in the tubing connecting the furnace to the pressure meter is not adequate to make the necessary corrections to the pressure for thermal transpiration and recombination. However, the pressure at the pressure meter is directly proportional to the atomic-hydrogen density in the furnace as long as the temperature of the furnace and environment do not change.

With the target furnace cold, the energy-loss spectrum of molecular hydrogen is obtained when the hydrogen gas is introduced into the target cell. The spectrum of molecular hydrogen is shown in Fig. 1. The spectrum as a result of the Lyman- $\alpha$  bands<sup>10</sup> displays a broad peak at 12.5 eV. This spectrum starts at about 11.2 eV energy loss, reaches a peak at 12.5 eV, and decreases monotonically at higher energy losses. As the furnace is heated, the spectrum begins to change. A new peak at 10.2 eV energy loss that is attributed to the excitation of atomic hydrogen to the  $n=2$  state appears and increases while the peak at 12.5 eV changes shape and decreases. However, in this spectrum, the peak near 12.5 eV is now primarily due to the excitation of atomic hydrogen to the  $n=3$  and  $n=4$  states. The monotonically decreasing tail is due to excitations of higher discrete states and the ionization continuum. The spectrum observed at high furnace temperatures is also shown in Fig. 1.

The determination of the cross section for excitation to the  $n=2$  state does not depend on the complete dissociation of the molecular hydrogen, because the 10.2-eV peak is well resolved from the molecular peak. However, the broad peak at 12.5 eV may contain a small contribution from the Lyman- $\alpha$  bands of any residual molecular hydrogen in the furnace. As the furnace temperature is in-

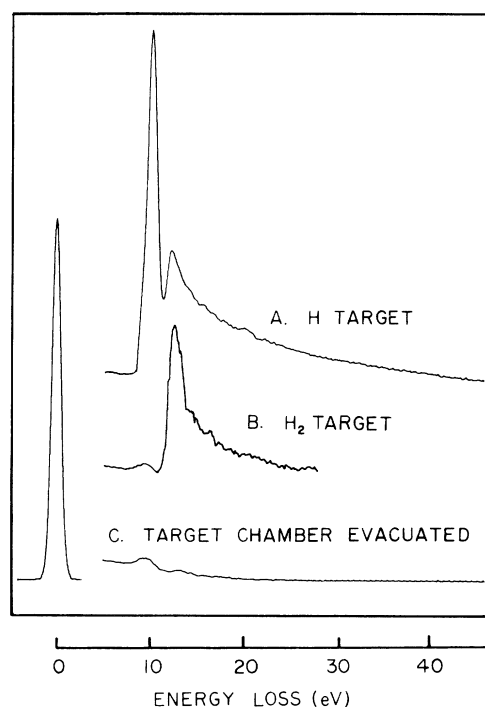


FIG. 1. Raw-data spectra for 50-keV protons: A, atomic-hydrogen target; B, molecular-hydrogen target; and C, target chamber evacuated.

creased, the atomic hydrogen increases while the molecular hydrogen is depleted and the molecular contribution to the 12.5-eV energy-loss peak is reduced. The ratio of the peak at 10.2 eV to the peak at 12.5 eV can therefore be used as an indication of the amount of residual molecular hydrogen present in the target furnace. This ratio increases with temperature until it reaches a plateau. Raising the furnace temperature further does not make any observable changes in spectral shape, indicating that the molecular hydrogen no longer makes a significant contribution to the spectrum. From these considerations, the molecular fraction is estimated to be no more than 3% and is probably less than 1% during the data acquisition period. This limit on the molecular fraction is consistent with estimates based on the pressure and temperature conditions in the furnace.

At each impact energy, spectra are obtained both with and without atomic hydrogen in the target furnace. The spectra are taken by recording the ion current at 0.1-eV intervals in energy loss. The pressure at the time of the reading is also digitally recorded. Effects caused by small differences between the set pressure and the measured pressure are corrected during data analysis. These corrections are typically 2% or less. If the pressure correction to any data point exceeds 15%, the data run

is automatically aborted. Typically six energy-loss spectra are obtained with gas in the target chamber, and six spectra are obtained without gas at each impact energy. The average of the spectra taken with no gas in the furnace is scaled to take into account the loss of protons resulting from the charge changing effects and is then subtracted point by point from the average of the spectra with gas in the chamber. Figure 2 shows an averaged spectrum which has been corrected for background in this manner.

Consecutive sets of these energy-loss spectra are taken at various energies of the incident proton from 200 down to 15 keV and back up to 200 keV. The pressure and temperature in the target furnace are held constant during the entire series, and thus the atomic-hydrogen density in the furnace is also constant. This technique makes it possible to normalize the entire series of spectra to a theoretical cross section. (The normalization effectively determines the density of atomic hydrogen in the target furnace.)

To obtain cross sections, the current readings are first reduced to the form of a differential cross section,<sup>11</sup>

$$\frac{dR(\xi)}{d\xi} = \frac{1}{nl} \frac{I(\xi)}{I_f}.$$

In this equation  $l$  is the length of the collision chamber,  $n$  the target-gas density,  $I_f$  the total current obtained by integrating the elastic peak

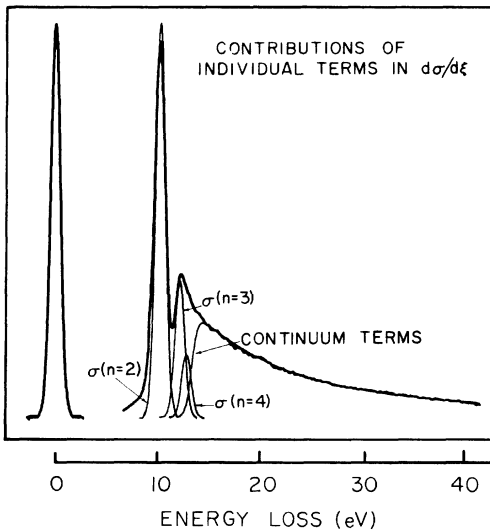


FIG. 2. Average energy-loss spectrum. The heavy curve is the average of six spectra from which the background has been subtracted (see text). The light lines are the convolution of the individual terms in the calculated differential cross section with the resolution function.

of the spectrum, which is centered at zero energy loss, and  $I(\xi)$  the proton current measured at an energy loss  $\xi$ .

The spectrum  $dR(\xi)/d\xi$  is a convolution of the energy resolution function  $\Phi(\xi)$  with the cross-section differential in energy loss,  $d\sigma(\xi)/d\xi$ :

$$\frac{dR(\xi)}{d\xi} = \int \frac{d\sigma(\xi')}{d\xi'} \Phi(\xi - \xi') d\xi'. \quad (1)$$

The resolution function  $\Phi(\xi)$  has the profile shown for the zero-energy-loss peak and a magnitude such that  $\int \Phi(\xi) d\xi = 1$ . The composite differential cross section is assumed to have the form

$$\frac{d\sigma(\xi')}{d\xi'} = \sum_n \sigma_n \delta(\xi' - \xi_n) + \sum_m A_m \xi'^m. \quad (2)$$

The term  $\sigma_n$  is the cross section for excitation to the  $n$ th discrete state located at the energy loss  $\xi_n$ . The summation over  $n$  describes excitation to the  $n=2, 3, 4, 5, 6, \dots$  discrete states in which  $\xi_2 = 10.200$ ,  $\xi_3 = 12.084$ ,  $\xi_4 = 12.745$ ,  $\xi_5 = 13.051$ ,  $\xi_6 = 13.217$  eV, and so on. Because the energy width of these states is very narrow on our energy-loss scale, a Dirac  $\delta$  function centered at  $\xi_n$  is used to describe them. The second term,  $\sum_m A_m \xi'^m$ , is a polynomial series used to represent the continuum and discrete states so closely spaced as to appear as a continuum in the spectrum. The coefficient  $A_m$  is equal to 0 if  $\xi'$  is less than  $\xi_I$ , in which  $\xi_I$  is the energy of the first discrete state not explicitly included in the summation over  $n$ .

The exponents  $m$  are chosen to fit the high-energy tail. Typically, the most satisfactory fits to the data are achieved when  $m$  is given two or three values ranging from  $-3$  to  $-5$ . (Note that the Born cross section is approximately proportional to  $\xi^{-4.5}$ .) The coefficients in Eq. (2) are obtained by a least-squares fit, which minimizes  $D$ :

$$D = \sum_i \left( \int \Phi(\xi_i - \xi') \frac{d\sigma(\xi')}{d\xi'} d\xi' - \frac{dR(\xi_i)}{d\xi} \right)^2, \quad (3)$$

in which the discrete  $\xi_i$  are the energy-loss values at the data points on the spectrum. Because the continuum and discrete states both contribute to some parts of the observed spectrum, it is necessary to fit both discrete and continuum states simultaneously.

Figure 2 shows a corrected spectrum and the calculated fit. The fitting process yields values of  $\sigma_2$  and  $\sigma_3$ , which are generally insensitive to the number of discrete states chosen and to inaccurate fitting of the continuum portion of the curve. However,  $\sigma_4$  is more sensitive and requires an accurate fit to the continuum states.

### III. DATA

Cross-section data for excitation of atomic hydrogen to the  $n=3$  state by protons are shown in Fig. 3. The error bars represent only the random error. More than 1700 spectra were analyzed to obtain this curve. The data were taken at three different time periods and were analyzed in two slightly different ways. The first set of data was obtained before the complete least-squares computer analysis was available. For these data,  $\sigma_3$  was obtained by simply integrating the instrumental profile over the region corresponding to the  $n=3$  states. The second and third groups of data were analyzed by using the fitting process described above. In the second group of data, each spectrum was taken to a 45 eV energy loss. In the third group of data, each spectrum was taken to a 25 eV energy loss. Hence the spectra used in the third group do not include as much of the ionization continuum. The analyzed results from the three groups of data are in excellent agreement, and no obvious systematic difference was found between the three groups.

As discussed previously, the relative shapes of the cross-section curves are reasonably accurate because of the method used to take the data. To obtain absolute cross sections, one of the cross-section curves must be normalized at one incident proton energy to some theoretical value. The data have been normalized to the Born-approximation

calculation<sup>12</sup> of  $\sigma_2$  at 200 keV proton energy.<sup>5</sup> The  $\sigma_2$  cross section is used because the  $\sigma_2$  energy-loss peak is well resolved from the other spectral features, is free from possible errors resulting from residual molecular hydrogen, and has the largest signal-to-noise ratio of the measured cross sections. The choice of normalizing to the Born-approximation calculation was made at the time of the preliminary publication of the  $\sigma_2$  data, and this normalization has been retained for consistency. As will be discussed below, the best fit to the data is given by the Glauber-approximation calculations.<sup>13,14</sup> Also, comparison with proton-helium collisions<sup>15,16</sup> indicates that the Glauber-approximation calculations are more reliable at lower proton impact energies than Born-approximation calculations. These considerations suggest that it might have been better to normalize to the Glauber calculation; however, the reader may easily renormalize the data if he wishes.

The cross-section data for excitation to the  $n=4$  state is based entirely on the "long" data group. They are less precise, because the amount of data is smaller and the cross sections are more susceptible to noise. The data are shown in Fig. 4.

The results for  $\sigma_3$  and  $\sigma_4$  have not been corrected for the contribution of the residual molecular hydrogen in the target furnace. Any residual molecular hydrogen does not affect the cross section for excitation to the  $n=2$  state, because the energy-loss spectrum of hydrogen is zero at 10.2 eV en-

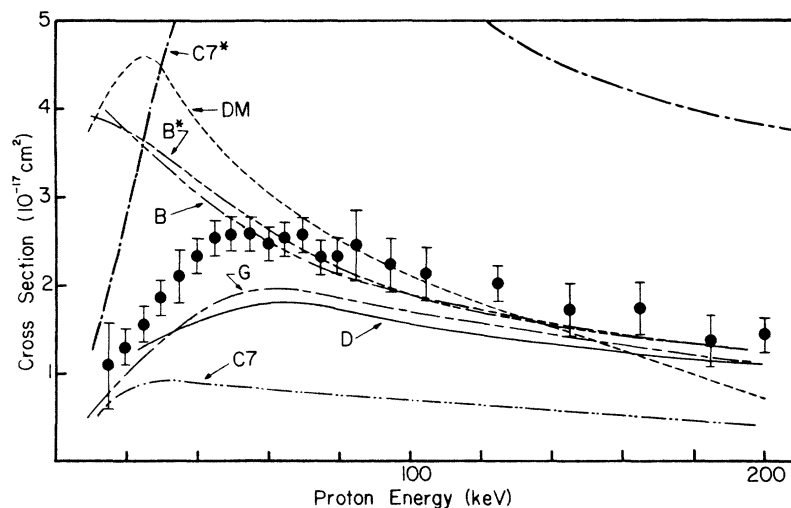


FIG. 3. Cross section for excitation of atomic hydrogen to the  $n=3$  state by proton impact. The solid circles are our data normalized as discussed in the text. Curve B is a Born theoretical calculation (Ref. 12). Curve B\* is a Born approximation calculation in the impact-parameter formulation (Ref. 18). Curve C7 is a seven-state close-coupling calculation (Ref. 17). Curve C7\* is a seven-state close-coupling calculation including pseudostates (Ref. 20). Curve D is a distortion calculation (Refs. 19 and 22). Curve DM is a 20-state diagonalization-method calculation (Ref. 21). Curve G is a Glauber-approximation calculation (Refs. 13 and 14).

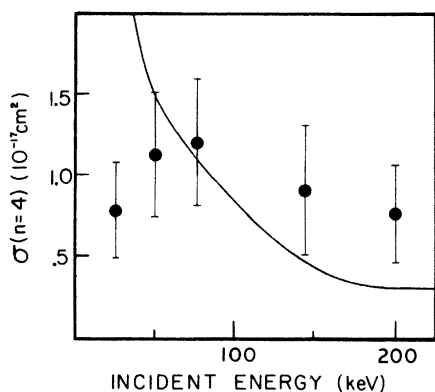


FIG. 4. Cross section for excitation of atomic hydrogen to the  $n=4$  state by proton impact. The solid circles are our data normalized as discussed in the text. The theoretical curve is the 20-state diagonalization method calculation of Baye and Heenen (Ref. 21).

ergy loss. However, molecular-hydrogen contamination in the target furnace has an effect on the cross sections for the  $n=3$  and 4 excitation. A 3% molecular-hydrogen contamination in the collision chamber would make it necessary to reduce  $\sigma_3$  by 3% and  $\sigma_4$  by 8% at all incident energies. However, as noted above, we believe 3% to be an upper limit on the fraction of molecular hydrogen.

Table I lists the numerical values for the cross sections for excitation of atomic hydrogen to the  $n=2, 3$ , and 4 states. The uncertainties listed include only random errors. The data are normalized to the Born-approximation calculation<sup>12</sup> for excitation of atomic hydrogen from the ground state to the  $n=2$  state by 200-keV protons,  $\sigma_2(200 \text{ keV}) = 6.637 \times 10^{-17} \text{ cm}^2$ . These data may be renormalized to the Glauber-approximation calculation<sup>13, 14</sup> for  $\sigma_2(200 \text{ keV})$  by multiplying the data by 0.9218.

#### IV. COMPARISONS WITH THEORY

A large number of calculations for excitation of atomic hydrogen by protons have been performed because of the fundamental nature of the proton-atomic-hydrogen collision. Most of these calculations deal with the excitation to the  $n=2$  state. The results for  $\sigma_2$  reported here involve more data and better statistics than the preliminary report<sup>5</sup>; however, the comparison with theory is not changed. These observations may be summarized by noting the satisfactory agreement in the shape of the cross-section curves of the data and the Glauber-approximation calculation of Franco and Thomas.<sup>13</sup> The distorted-wave eikonal calculation also gives a satisfactory agreement. The best agreement in magnitude near the maximum in the cross-section curve is given by the seven-state impact-param-

TABLE I. Cross section for the excitation of atomic hydrogen,  $\text{H}^+ + \text{H}(1s) \rightarrow \text{H}^+ + \text{H}^*$ . The uncertainties shown are rms random-error calculations. They do not include any contribution from the normalization procedure. All data were normalized by using the Born theoretical calculation for excitation of atomic hydrogen to the  $n=2$  state by 200-keV protons, taken from Bates and Griffing (Ref. 12) [ $\sigma(n=2) = 6.637 \times 10^{-17} \text{ cm}^2$  at 200 keV].

Energy (keV)	Cross section ( $10^{-17} \text{ cm}^2$ )		
	$n=2$	$n=3$	$n=4$
15	3.44±0.40	1.1±0.5	
20	5.36±0.20	1.3±0.2	
25	6.63±0.44	1.55±0.2	0.78±0.3
30	7.86±0.50	1.86±0.2	
35	8.47±0.78	2.11±0.3	
40	9.64±0.83	2.35±0.2	
45	9.90±0.97	2.52±0.2	
50	10.53±0.64	2.58±0.2	1.13±0.4
55	10.59±0.25	2.59±0.2	
60	10.74±0.64	2.47±0.2	
65	10.19±0.66	2.53±0.2	
70	10.26±0.84	2.59±0.2	
75	10.26±0.27	2.31±0.2	1.21±0.4
80	9.75±0.38	2.32±0.2	
85	9.47±0.70	2.47±0.4	
95	9.32±0.55	2.22±0.3	
105	8.88±0.29	2.13±0.3	
125	8.47±0.24	2.01±0.2	
145	7.75±0.58	1.72±0.3	0.92±0.4
165	7.27±0.31	1.73±0.3	
185	6.87±0.20	1.38±0.3	
200	6.637±0.35	1.41±0.2	0.77±0.3

eter coupled-state calculation of Rapp and Dinwiddie.<sup>17</sup> This theory does not provide as good agreement in the curve shape as the Glauber approximation.

Figure 3 shows various theoretical calculations and the data for  $\sigma_3$ . The agreement between experiment and theory is mixed. The data are bracketed by the calculations. The Born calculations labeled B (Ref. 12) and B\* (Ref. 18) are in close accord with the data at energies greater than 80 keV, but the maximum in the Born calculations is too high and occurs at too low an energy.

The measured  $\sigma_3$  value includes excitation to the  $3s, 3p$ , and  $3d$  levels. The  $1s$  to  $3d$  excitation represents a small fraction of the excitation to the  $n=3$  level and was not calculated by several of the theorists. For comparison with our data, the cross section for excitation to the  $3d$  level calculated by Chaudhuri *et al.*<sup>19</sup> was added to the calculations of Rapp and Dinwiddie<sup>17</sup> and Cheshire *et al.*<sup>20</sup> The seven-state close-coupling calculation by Rapp and Dinwiddie<sup>17</sup> includes charge exchange channels, but the close agreement between this calculation and experiment obtained for  $\sigma_2$  is

not obtained in the case of  $\sigma_3$ . This result is not unexpected, because in a close-coupling calculation the last channels included might be expected to absorb the effects of any missing channels and hence display the least accuracy.

This effect is even more noticeable in the seven-state close-coupling calculation of Cheshire *et al.*<sup>20</sup> This calculation includes pseudostates to represent coupling to the higher states. The inclusion of these pseudostates provides an excellent representation of the excitation of atomic hydrogen to the  $n=2$  states at low impact energies, <30 keV. Their inclusion, however, results in a poorer fit to the  $n=2$  data at intermediate (35–125 keV) energies.<sup>5</sup> The fit to the  $n=3$  data is not adequate. The marked difference between the coupled-state calculation with and without the pseudostates indicates that the contribution of the pseudostates can be very large and can seriously distort the results. It should be explained that the pseudostates used by Cheshire *et al.*<sup>20</sup> were representations of the  $3s$  and  $3p$  states designed to give better results for the charge transfer and the  $n=2$  excitation of hydrogen. Thus their cross section for the  $n=3$  excitation of hydrogen really represents an excitation to their  $n=3$  pseudostate and may not represent an excitation to the actual  $n=3$  state of hydrogen. This may account for the poor agreement.

The 20-state diagonalization method, curve DM, in Fig. 3, applied by Baye and Heenen<sup>21</sup> gives results that are lower than the data at high energies and higher at the low energies. The good agreement between this theory and experiment for protons incident on helium<sup>15</sup> is not duplicated for protons on atomic hydrogen.

While the theoretical values are lower than the experimental data, the best agreement between experiment and theory for the shape of the  $\sigma_3$  curve is given by the distortion calculation of Chaudhuri *et al.*<sup>19,22</sup> and the Glauber calculation using the  $1s-3s$  and  $1s-3p$  cross sections of Franco and Thomas<sup>13</sup> and the  $1s-3d$  excitation cross section of Bhadra and Ghosh.<sup>14</sup> The agreement between these two calculations is not unexpected. Shields and Peacher<sup>23</sup> have shown that an eikonal calculation and a two-state impact-parameter calculation give similar results for the total cross section as a function of incident projectile energy.

Figure 4 shows the data for excitation of atomic hydrogen to the  $n=4$  state. Also shown for comparison are the calculations of Baye and Heenen,<sup>21</sup> which are the only available theoretical values for  $\sigma_4$ . The agreement is not good. In spite of the uncertainties in our fitting and normalization technique, the shape of the spectra places limits on the values that the  $n=4$  can take without distorting

the observed spectral shape. If the theoretical value of the  $n=4$  cross section at 25 keV were correct, the energy-loss spectrum for 25-keV protons incident on atomic hydrogen would look much different than it does.

## V. DISCUSSION

The data for excitation of atomic hydrogen to the  $n=3$  and  $n=4$  states are the only ones available. The  $\sigma_2$ ,  $\sigma_3$ , and  $\sigma_4$  cross sections are all very similar in shape. They increase with proton energy to a peak at 60 keV and then decrease at higher energies. This major feature of the cross sections can be inferred from the spectra themselves. The spectra taken at various proton energies look very similar, suggesting that the relative magnitudes of the cross sections are not strongly energy dependent.

The relative shape of the cross-section curves for  $\sigma_2$ ,  $\sigma_3$ , and  $\sigma_4$  can be seen in Fig. 5. In this figure both data and theory have been normalized to unity at 200 keV. The figure shows that the curve shapes for  $\sigma_2$ ,  $\sigma_3$ , and  $\sigma_4$  are very similar. Also shown are the Glauber calculations for  $\sigma_2$

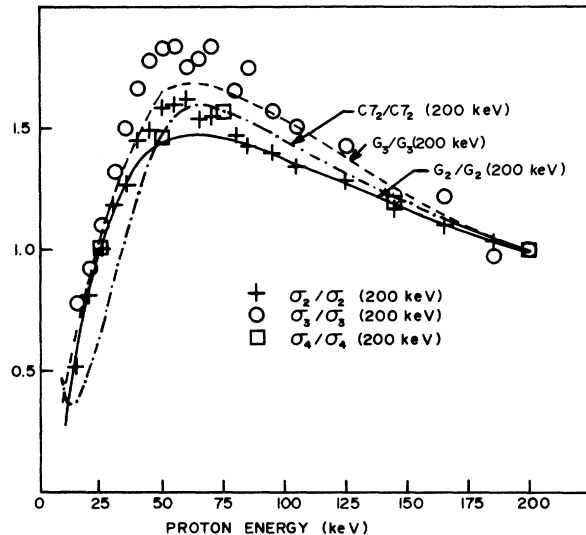


FIG. 5. Relative cross sections for excitation of atomic hydrogen to the  $n=2$ , 3, and 4 states. All of the data and theory curves have been set equal to 1 at 200 keV. +, relative cross section for excitation to the  $n=2$  state,  $\sigma_2$ ;  $\circ$ , relative cross section for excitation to the  $n=3$  state,  $\sigma_3$ ;  $\square$ , relative cross section for excitation to the  $n=4$  state,  $\sigma_4$ . Curve  $G_2$  is the relative Glauber-approximation calculation of  $\sigma_2$  by Franco and Thomas (Ref. 13). Curve  $G_3$  is the relative Glauber-approximation calculation of  $\sigma_3$  by Franco and Thomas (Ref. 13) including the  $1s-3d$  excitation cross section of Bhadra and Ghosh (Ref. 14). Curve  $C7_2$  is the relative seven-state close-coupling calculation by Rapp and Dinwiddie (Ref. 17) for  $\sigma_2$ .

(Ref. 13) and  $\sigma_3$  (Refs. 13 and 14) and the close-coupling calculation for  $\sigma_2$  (Ref. 17). When the Glauber-theory calculations and the data are normalized to the same value, the excellent agreement in curve shape can be seen. Both experiment and theory produce a more pronounced peak in the  $n=3$  cross section than in the  $n=2$  cross section. This effect is not large but appears to be real.

Excitation to the  $n=3$  and  $n=4$  states does not result in resolved features in the energy-loss spectra. However, the spectra do contain the information required to calculate the cross sections for excitation of atomic hydrogen to these higher states. The plotting of numerically convoluted alternate cross sections shows that if the cross sections for these states were significantly changed from the observed values, the resulting energy-loss spectra would be changed in shape. Any sizable fraction of molecular hydrogen in the

target furnace would also affect the shape of the energy-loss spectra.

The good agreement achieved by the relatively simple Glauber and distortion calculations for excitation of atomic hydrogen to both the  $n=2$  (Ref. 5) and  $n=3$  states suggests that calculations in these approximations for the  $n=4$  state excitation would be fruitful. The Glauber and the eikonal distorted-wave calculations will give very similar results, but it would also be very interesting to be able to compare the predicted curve shapes with the experimental results for the  $n=3$  and 4 excitations.

#### ACKNOWLEDGMENTS

The assistance of E. B. Hale in preparing the manuscript is very much appreciated.

---

\*Work supported by the National Science Foundation.

<sup>1</sup>R. F. Stebbings, R. A. Young, C. L. Oxley, and H. Ehrhardt, *Phys. Rev.* **138**, A1312 (1965).

<sup>2</sup>R. A. Young, R. F. Stebbings, and J. W. McGowan, *Phys. Rev.* **171**, 85 (1968).

<sup>3</sup>J. T. Morgan, J. Geddes, and H. B. Gilbody, *J. Phys.* **B 6**, 2118 (1973).

<sup>4</sup>T. Kondow, R. J. Girnius, Y. P. Chong, and W. L. Fite, *Phys. Rev. A* **10**, 1167 (1974).

<sup>5</sup>J. T. Park, J. E. Aldag, and J. M. George, *Phys. Rev. Lett.* **34**, 1253 (1975).

<sup>6</sup>J. T. Park and F. D. Schowengerdt, *Rev. Sci. Instrum.* **40**, 753 (1969).

<sup>7</sup>V. Pol, W. Kauppila, and J. T. Park, *Phys. Rev. A* **8**, 2990 (1973).

<sup>8</sup>G. W. York, Jr., J. T. Park, J. J. Miskinis, D. H. Crandall, and V. Pol, *Rev. Sci. Instrum.* **43**, 230 (1972).

<sup>9</sup>F. D. Schowengerdt and J. T. Park, *Phys. Rev. A* **1**, 848 (1970).

<sup>10</sup>V. Pol, J. George, and J. T. Park, *Bull. Am. Phys. Soc.* **18**, 1517 (1973).

<sup>11</sup>D. R. Schoonover and J. T. Park, *Phys. Rev. A* **3**, 228 (1971).

<sup>12</sup>D. R. Bates and G. Griffing, *Proc. Phys. Soc. London* **66**, 64 (1953).

<sup>13</sup>V. Franco and B. K. Thomas, *Phys. Rev. A* **4**, 945 (1971).

<sup>14</sup>K. Bhadra and A. S. Ghosh, *Phys. Rev. Lett.* **26**, 737 (1971).

<sup>15</sup>R. Hippler and K. H. Schartner, *J. Phys.* **B 7**, 618 (1974).

<sup>16</sup>C. J. Joachain and R. Vanderpoorten, *J. Phys.* **B 7**, 817 (1974).

<sup>17</sup>D. Rapp and D. Dinwiddie, *J. Chem. Phys.* **57**, 4919 (1972).

<sup>18</sup>J. van den Bos and F. J. DeHeer, *Physica (Utr.)* **34**, 333 (1967).

<sup>19</sup>J. Chaudhuri, D. M. Bhattacharya, and N. Sil, *J. Phys.* **B 7**, 1027 (1974).

<sup>20</sup>I. M. Cheshire, D. F. Gallaher, and A. J. Taylor, *J. Phys.* **B 3**, 813 (1970).

<sup>21</sup>D. Baye and P. H. Heenen, *J. Phys.* **B 6**, 105 (1973).

<sup>22</sup>J. Chaudhuri, D. M. Bhattacharya, and N. Sil, *J. Phys.* **B 5**, 525 (1972).

<sup>23</sup>R. H. Shields and J. L. Peacher, *Phys. Rev. A* **9**, 743 (1974).